Journal of Molecular Graphics and Modelling 53 (2014) 112–117

Contents lists available at ScienceDirect

Journal of Molecular Graphics and Modelling

journal homepage: www.elsevier.com/locate/JMGM

Functionalized graphene as a nanostructured membrane for removal of copper and mercury from aqueous solution: A molecular dynamics simulation study

Jafar Azamat [a], Alireza Khataee [a,*], Sang Woo Joo [b,**]

[a] Research Laboratory of Advanced Water and Wastewater Treatment Processes, Department of Applied Chemistry, Faculty of Chemistry, University of Tabriz, 51666-14766 Tabriz, Iran
[b] School of Mechanical Engineering, Yeungnam University, Gyeongsan 712-749, Republic of Korea

ARTICLE INFO

Article history:
Accepted 21 July 2014
Available online 30 July 2014

Keywords:
Nanostructured membrane
Graphene
Potential of mean force
Molecular dynamics simulation
Desalination

ABSTRACT

The purpose of the present study was to investigate the removal of copper and mercury using functionalized graphene as a nanostructured membrane. The molecular dynamics simulation method was used to investigate the removal ability of these ions from aqueous solution using functionalized graphene membrane. The studied systems included a functionalized graphene membrane which was placed in the aqueous ionic solution of $CuCl_2$ and $HgCl_2$. An external electrical field was applied along the *z* axis of the system. The results indicated that the application of electrical field on the system caused the desired ions to pass through the functionalized graphene membrane. The Fluorinated pore (F-pore) terminated graphene selectively conducted Cu^{2+} and Hg^{2+} ions. The calculation of the potential of mean force of ions revealed that Cu^{2+} and Hg^{2+} ions face a relatively small energy barrier and could not pass through the F-pore graphene unless an external electrical field was applied upon them. In contrast, the energy barrier for the Cl^- ion was large and it could not pass through the F-pore graphene. The findings of the study indicate that the permeation of ions across the graphene was a function of applied electrical fields. The findings of the present study are based on the detailed analysis and consideration of potential of mean force and radial distribution function curves.

1. Introduction

The pollution of water by heavy metals is considered to be a serious concern around the world throughout the past decade. Some heavy metals can be toxic and harmful for human life. Some of industrial wastewater may contain toxic heavy metals. Elements which are toxic for humans and the environment range from copper, mercury, chromium, lead, manganese, cadmium, nickel, zinc to iron. In case the concentration of such heavy metals increases beyond the permitted limit in wastewater, they must be eliminated from wastewater since these heavy metals in water can cause many worrying problems. Hence, different technologies and measures should be taken to prevent the increase of such metals. The experimental procedures which might be applied to get rid of heavy metals include precipitation, flocculation, ion exchange, reverse osmosis [1–3], electrochemical operation and biological treatment [4,5]. One more technique which might be considered is to make use of the technology of nanostructured membranes. Nanostructured membranes offer some technologies for separating ions. The flux across a membrane increases based on the size of a pore created in the membrane. One nanostructured membrane is graphene which has unique properties such as ultimate thinness, flexibility, chemical stability, and mechanical strength [6–8]. Thanks to these outstanding properties, graphene can be considered as a highly appropriate choice for removing ion. Since the isolation of graphene [9], it has been a research agenda for many theoretical [10] and empirical research studies [11]. Specifically, functionalized graphene membranes as well as nanoporous membranes [12–15] have unique properties and applications [7,16–23]. Nanoscale pores can be introduced in graphene with unsaturated carbon atoms at the pore edge which are passivated by chemical functional groups. Recently, several experimental studies have been developed to create pores in graphene, [24–26]. Although numerous studies have found many applications of graphene in several areas such as DNA sequencing and gas separation [27,28], the role and significance of this material for removing heavy metal

* Corresponding author. Tel.: +98 411 3393165; fax: +98 411 3340191.
** Corresponding author. Tel.: +82 53 810 2568.
E-mail addresses: a_khataee@tabrizu.ac.ir, ar_khataee@yahoo.com (A. Khataee), swjoo@yu.ac.kr (S.W. Joo).

http://dx.doi.org/10.1016/j.jmgm.2014.07.013
1093-3263/

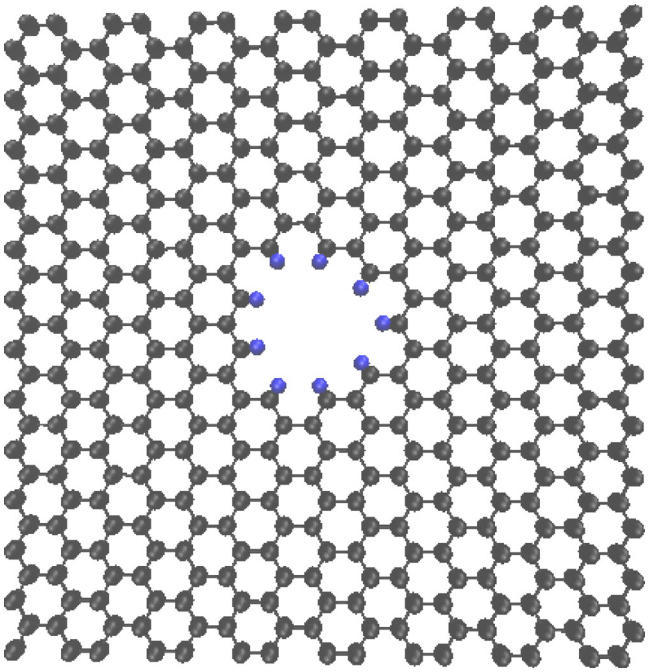

Fig. 1. Functionalized graphene membranes as a nanostructured membrane (black: carbon; blue: fluoride). (For interpretation of the references to color in this figure legend, the reader is referred to the web version of the article.)

from aqueous solutions remains unexplored and is considered to be a research gap. Therefore, it may be speculated that this membrane can potentially act as a filter for ion separation. Graphene is assumed to show high selectivity through molecular size exclusion effects and at the same time it has high permeability due to its very little thickness. A graphene without any defects does not have any pores and hence is not permeable to gases [29]; this is attributed to the fact that the electron density of its aromatic rings is enough to repel atoms trying to pass through this membrane. Hence, to achieve ion permeability, it is necessary to drill pores in the graphene by a chemical or thermal treatment [30,31]. It has been acknowledged that cavitary graphenes are highly efficient membrane materials for ion, gas and nanoparticle separation [32,33].

To the best of researchers' knowledge, no studies have been conducted on removing copper and mercury ions by functionalized graphene. Thus, the researchers intended to address this research lacuna in the present study. That is, molecular dynamics (MD) simulations of functionalized graphene was used to remove heavy metals from aqueous solution under the application of electrical field. How ion removal changes based on pore chemistry and applied electrical field was investigated in this paper. In this study, a functionalized graphene was designed and it was found that this grapheme can effectively separate heavy metals from water. The researchers expect that the findings of the present study can be used as a research initiative and framework for designing energy-efficient graphene-based tools for heavy metal separation.

2. Computational methods and details

The full view of the functionalized graphene as a nanostructured membrane is shown in Fig. 1. A full geometric optimization of functionalized graphene was obtained by applying Density Functional Theory (DFT) method. DFT method was employed to obtain the optimized structure and atomic charges of functionalized graphene. These computations were done at the B3LYP

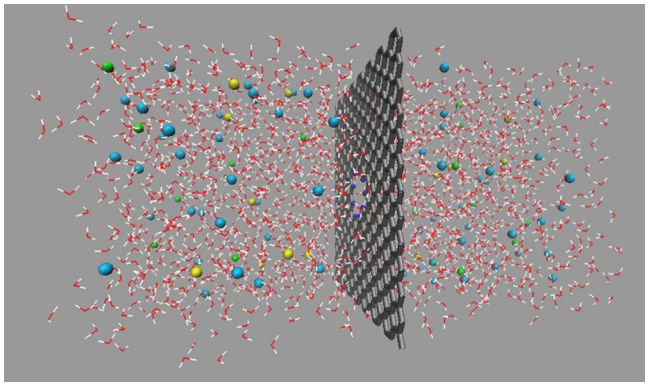

Fig. 2. A snapshot of the simulated system (black: carbon; blue: fluoride; green: Cu^{2+}; yellow: Hg^{2+}; cyan: Cl^{-}; red: O; white: H).

level of theory using 6-311G (2d, 2p) basis sets. All calculations were carried out using GAMESS-US package [34]. DFT has recently become the preferred method for systems, because it has some static correlation and suitable computational cost. Suitable computational cost term arises from the fact that DFT method depends on just three variables (x, y, z) while wave function theory for an n-electron molecule depends on $4n$ variables, three spatial coordinates and one spin coordinate, for each electron [35]. The definitions of exchange and correlation energies in DFT at least in current implementations are local or short-rang since they depend on the density at a given point and its immediate vicinity, *via* its derivatives [36]. But because of the nature of the exchange and correlation functional, DFT suffers the self-interaction error (SIE) of the electrons. SIE by exchange part for commonly used functionals simulates static correlation effects cannot be covered by single determinant wave function theory methods which is an advantage. Therefore DFT correlation includes only dynamic correlation and DFT exchange includes not only local exchange but also some static correlation, although the latter is present in an unspecified and uncontrolled way (SIE).

Long-range interactions for atomic species have been characterized with the Lennard–Jones potential [37,38]. Lennard–Jones parameters for carbon atoms included $\varepsilon = 0.2897$ kJ/mol and $\sigma = 3.39$ Å [39]. The water–graphene, water–ion and ion–graphene interaction parameters are derived by using Lorentz–Berthelot combining rules where $\sigma_{ij} = (\sigma_i + \sigma_j)/2$ and $\varepsilon_{ij} = (\varepsilon_{ij} \cdot \varepsilon_{ij})^{0.5}$. In this rule, ε_{ij} and σ_{ij} are regarded as the usual empirical Lennard–Jones parameters. The chemical agent which was used in this study to passivate each carbon in the graphene was a fluorine atom. Fluorinated pore (F-pore) was obtained by passivating each carbon at the pore edge with a fluorine atom. The researchers performed MD simulations with NAMD molecular dynamics package developed at the University of Illinois at Urbana-Champaign [40] as a previous work [41]. In this work, there was a 1 fs time-step with a 12 Å cut-off for van der Waals interactions and a Particle Mesh Ewald (PME) scheme [42] was used for electrostatic calculations; all the analysis scripts were composed locally using VMD, a visualization package available from UIUC visualized using VMD [43]. As it is illustrated in Fig. 2, the MD domain consisted of a functionalized graphene, water, and heavy metals (copper and mercury). The simulation box for all runs was 3 nm × 3 nm × 6 nm. Dimension of graphene sheet is 3 nm × 3 nm. The number atoms of graphene are 377 carbon atoms and 9 fluorine atoms. A repeated unit of graphene sheet was used for optimization of the functionalized graphene by DFT method.

In all the simulation period, an electrical field was applied in a direction which was perpendicular to the graphene membrane.

The applied electrical field is internal units of NAMD package. This is defined as Eq. (1):

$$e_{field} = -23.0605492\frac{V}{l_z} \quad (1)$$

where e_{field}, V and l_z are for the applied electrical field (in kcal/mol Å e), potential difference (in volt) and the size of the system along the z-axis (in Angstrom), respectively [44]. In this study, the parameters of CHARMM force field [45] and the TIP3P water model [46] were used for all simulations. The system was equilibrated for 1 ns to a constant temperature of 298 K and constant pressure of 1 bar. The temperature of the system was maintained at 298 K using a Langevin thermostat and a hybrid Nose–Hoover Langevin piston to maintain a pressure of 1 bar. The graphene was positioned in the middle of the box. The Carbon atoms in the graphene were held fixed during the simulations while water molecules and ions were allowed to move freely.

The current *vs.* electric field curve was generated for the studied systems using the results of simulations. Amount of current was calculated by Eq. (2):

$$I = \frac{n \cdot q}{\Delta t} \quad (2)$$

where n, q and Δt represent the average number of ions crossing the graphene membrane, the charge of the ion and the simulation time of one run, respectively.

The contrasting ion selectivity of the functionalized graphene can be clarified by the potential of mean force (PMF) [47]. The mean force distribution was obtained by sampling the force experienced by the ions which were placed at various positions along the z-axis. The z component of ions was held using a harmonic constraint of 12.5 kcal/mol Å^2 while the ion was free to move radially. This harmonic constraint was selected to give enough overlap between each window and its neighbors while constraining the ions enough to ensure adequate sampling of the entire reaction coordinate. Values smaller than 12.5 kcal/mol Å^2 were not appropriate. This simulation time for each window was checked for convergence of the results to ensure this was long enough. Each sampling window was run for 1 ns. The PMF of the specific ion moving through the graphene was computed by the umbrella sampling technique [48] and the data were analyzed using the weighted histogram analysis method (WHAM) [49].

3. Results and discussion

To investigate the permeation phenomenon, the researchers selected the MD simulations method which is considered to be an appropriate tool for the purpose of the study. The investigated system in this study included the heavy metals of copper and mercury and graphene membrane with the functionalized nanopore. Furthermore, the external electrical field was applied to examine the process of removing ions. Under the influence of this electrical field, a copper or mercury ion permeates from the functionalized pore of graphene. Although the respective pore has a radius large enough to accept copper and mercury ions, the results of MD simulations show that Cu^{2+} and Hg^{2+} ions permeate through this pore after a certain electrical field.

The heavy metal permeation from F-pore of graphene can be illustrated by calculating the PMF along the z-axis of the system. After averaging the force on the molecules at various z positions along the axis, the researchers computed the PMF by integrating the mean force along the z-axis; in doing so, the researchers placed an ion at various locations of the system along the z-axis and the umbrella sampling method was used. Fig. 3 reveals that the energy barrier for Cl^- is the highest. Also, the energy barrier for Hg^{2+} is higher than Cu^{2+}; this is due to the fact that the F-pore is terminated

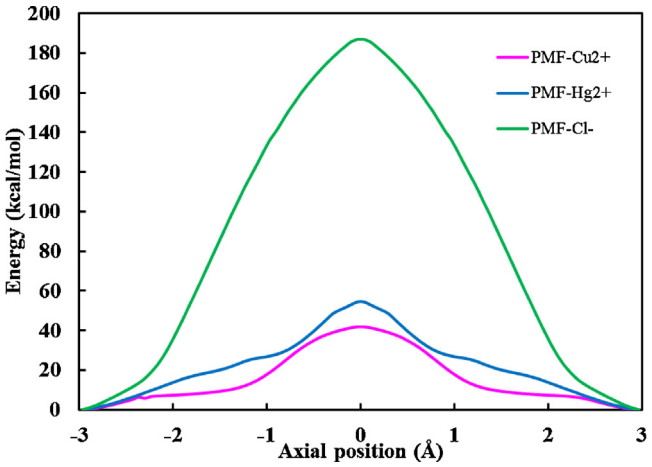

Fig. 3. The potential of mean force for Hg^{2+}, Cu^{2+}, and Cl^- ions.

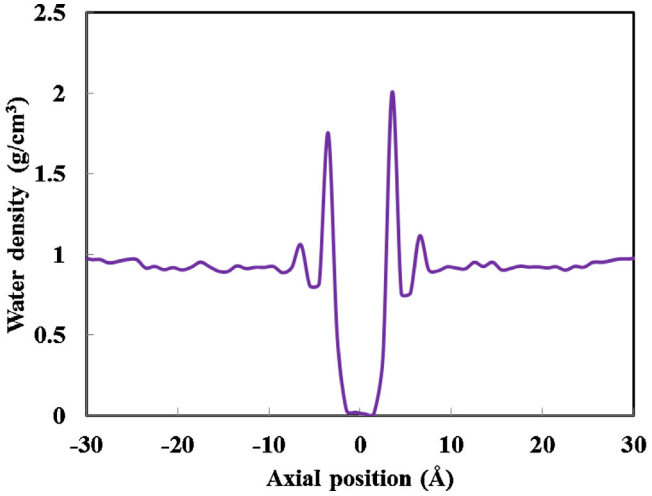

Fig. 4. Density profile of water molecules in simulated system.

by the negatively charged fluorine which favors the passage of cations. In other words, it should be maintained that the passing of ions would not be accomplished if the electrical field were not applied. Starting from 5 and 10 kcal/mol Å e for Cu^{2+} and Hg^{2+}, respectively, the Cu^{2+} and Hg^{2+} ions permeated from membrane.

In our systems, water molecules had different structures from it is of bulk water. The density of water was not identical in all systems. Fig. 4 depicts the density profile of water molecules in the simulated system; as shown in the figure, the density of water, on both sides of graphene is higher than that in the bulk. In this system, water molecules show the tendency to accumulate inside the region about ±3.5 Å around the graphene sheet. This structure is shown by two sharp peaks near the graphene. In the region near the graphene, layered structure was found in the water; however, the density of water in the region far from the graphene was 1 g/cm^3.

Fig. 5 shows the current–electrical field curve which was obtained by Eq. (2) for Cu^{2+} and Hg^{2+} ions. As the electrical field increases, the current increases. The increase in the current depends on the increase in the electrical field; this indicates that the number of ions passing across the graphene increased as a function of applying the electrical field (see Fig. 6) and as a result, the removal process was completely fulfilled.

Fig. 7 illustrates the retention time of the examined ions which is equal to the time of passing one ion through the graphene as a function of applying the electrical field. This figure reveals that the larger the electrical field is the smaller the retention time will be. In

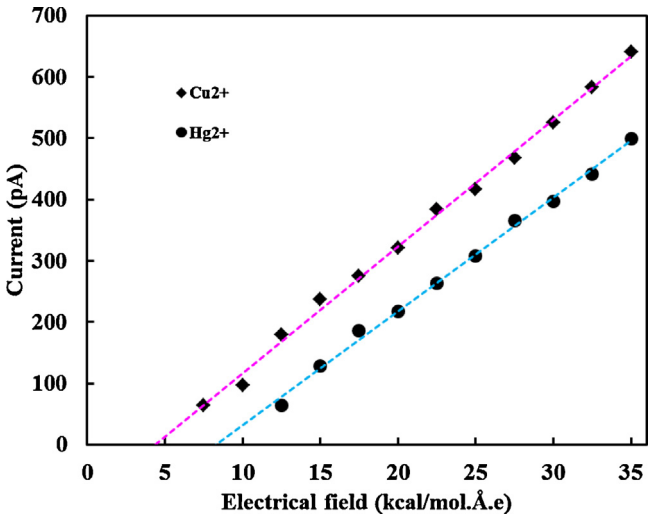

Fig. 5. Current–electrical field curves for Cu^{2+} and Hg^{2+} ions. Lines were obtained from linear regression.

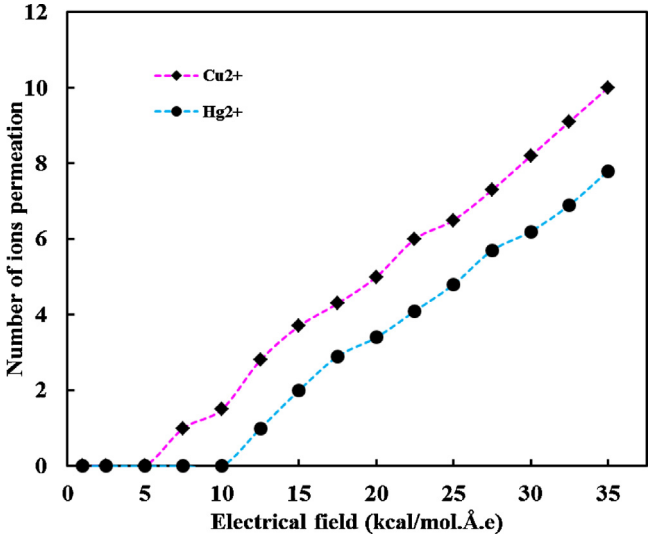

Fig. 6. The number of Cu^{2+} and Hg^{2+} ions passing through the membrane.

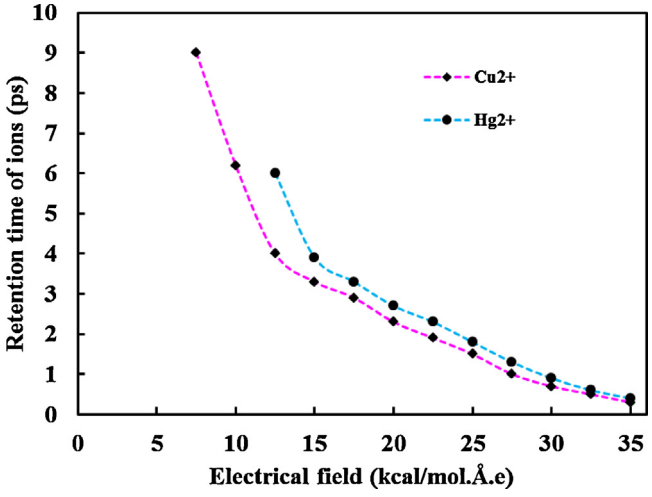

Fig. 7. Retention time for Cu^{2+} and Hg^{2+} ions at the applied electrical fields.

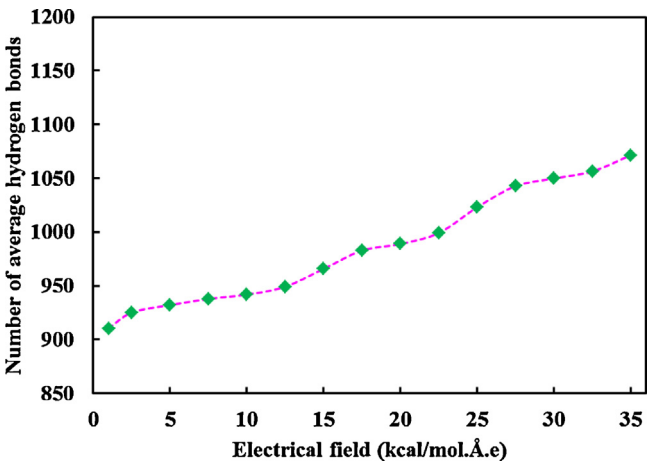

Fig. 8. Number of average hydrogen bonds at the applied electrical fields.

other words, it can be mentioned that ions were removed quickly from the aqueous solution by graphene membrane. Moreover, as it is shown in Fig. 7, the retention time for Hg^{2+} ion is larger than that for mercury ion; this is due to high energy barrier in PMF curve for mercury ion in comparison to the energy barrier of copper ion in PMF curve; hence, this is why the movement of mercury ions is slower than the movement of copper ions.

Fig. 8 shows the number of average hydrogen bonds (NAHB) at the applied electrical fields. As indicated in this figure, the NAHB will show an upside trend as the applied electrical field increases. Also, the dynamics of hydrogen bonds are considered to be an important parameter in our system. The dynamics of the hydrogen bonds are explained by the hydrogen bonding autocorrelation function ($C(t)$) of water molecules [50]. The $C(t)$ parameter is defined through Eq. (3):

$$C(t) = \frac{\langle h(0)h(t)\rangle}{\langle h\rangle} \tag{3}$$

where $h(t)$ is a hydrogen bond population operator which will be equal to 1 if a hydrogen bond is present at time t; otherwise, it will be zero. This parameter indicates the probability of hydrogen-bonded water molecules at time 0 to be hydrogen bonded at time t. Therefore, $C(t)$ reveals that how fast the hydrogen bonds of the system relaxed. The fast decrease of $C(t)$ in the graphene membrane suggests that the hydrogen-bonding process is relatively weak and is broken frequently. This process is intensified with a reduction in the electrical field; In other words, the breaking of hydrogen bonds

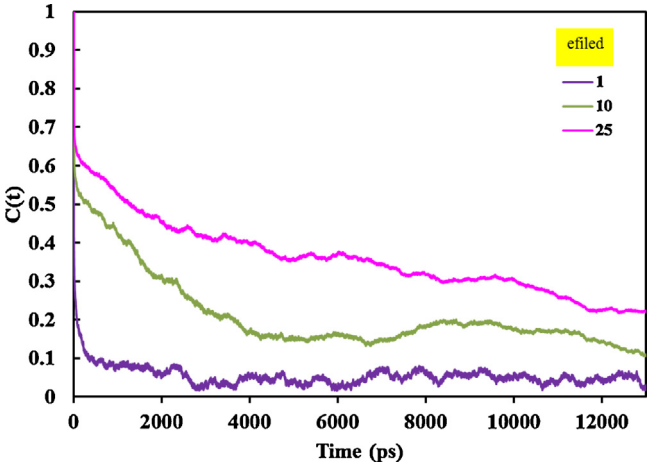

Fig. 9. Autocorrelation function of hydrogen bonds ($C(t)$).

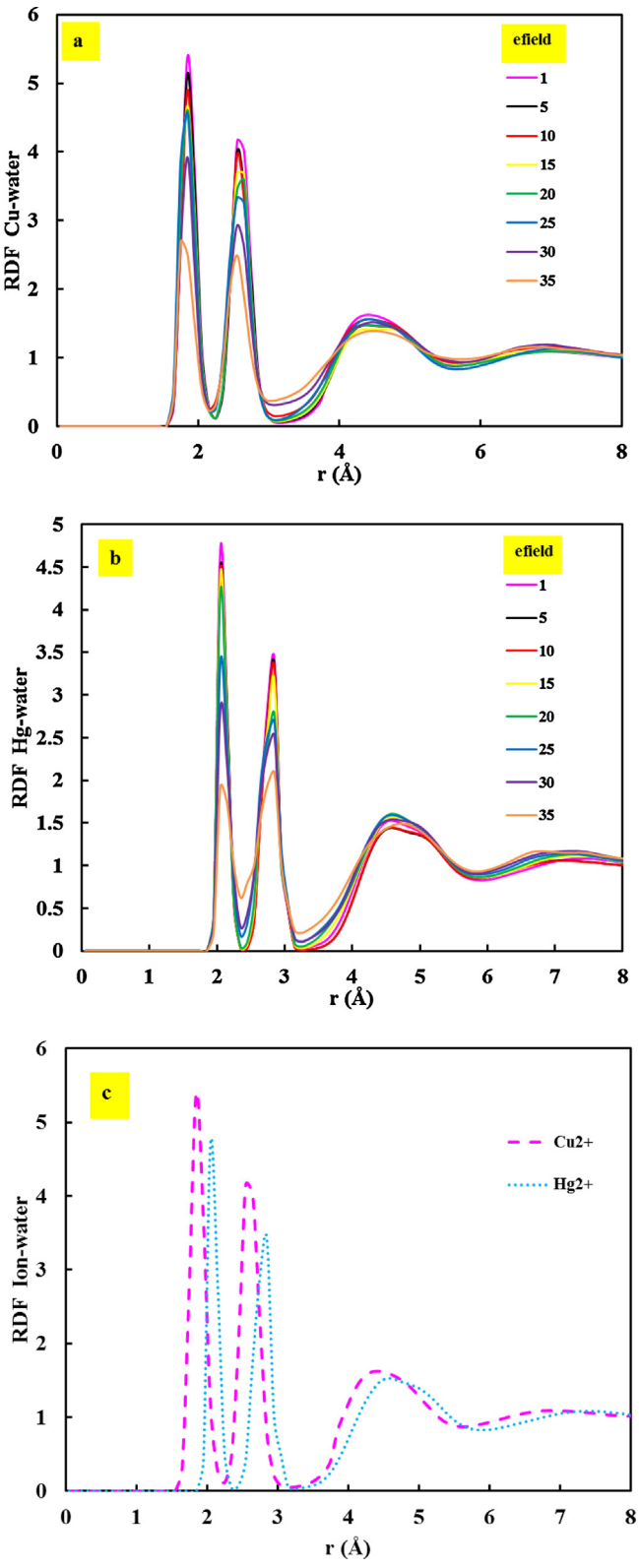

Fig. 10. Ion–water radial distribution function in the simulation box under various electrical fields: (a) RDF Cu^{2+}–water; (b) RDF Hg^{2+}–water; (c) comparison of Cu^{2+}–water and Hg^{2+}–water RDFs.

will decrease if the electrical field increases (see Fig. 9). This trend of increase or decrease in the number of hydrogen bonds can be also observed in Fig. 8. Indeed, Figs. 8 and 9 depict consistent patterns and changes in the respective processes.

To explain the structure change in each type of ion in the simulation box, the researchers calculated the radial distribution function (RDF) from the trajectories which were saved during the simulation. Fig. 10 illustrates the RDF between ion and water molecules under various electrical fields. Whereas Fig. 10(a) shows the RDF for Cu^{2+}–water, Fig. 10(b) illustrates the RDF for Hg^{2+}–water. It can be noted that RDF is zero for a short distance (less than atomic diameter) which is due to strong repulsive forces. For each ion, the position of the first maximum and the first minimum is similar in all the electrical fields. However, the magnitude of the first peak is different in each electrical field which indicates that the hydration number (number of water molecules in the first hydration shell) of the ions is different. Fig. 10(c) compares the position and magnitude of RDF peaks of Cu^{2+} and Hg^{2+}. As can be seen, position of Hg^{2+}–water RDF's is larger than position of Cu^{2+}–water RDF's but its magnitude is lower than that of copper. It was found that the height of the peaks decreases with an increase in the ion size. These results confirm the findings of other papers in the related literature [51–53].

4. Conclusion

In this paper, molecular dynamics simulations method was used to investigate the removing of ion by graphene as a nanostructured membrane. Removal of heavy metals from water is considered to be an important area of research in water technology. It was shown that the ion separation through graphene sheet happens in the presence of electrical field. By calculating the PMF for ions, the researchers showed that ions face an energy barrier and could not pass through F-pore graphene unless under the effect of applying an electrical field. The results show that Cu^{2+} and Hg^{2+} ions permeate through F-pore of graphene. According to the results, **it** can be mentioned that nanoscale pores in a single-layer graphene can effectively filter heavy metals from aqueous solutions.

Acknowledgments

The authors thank the Iranian National Science Foundation (INSF) for all of the support provided (No: 92030491). We also thank the University of Tabriz for the support provided. This work was funded by Grant 2011-0014246 from the National Research Foundation of Korea.

References

[1] P.M. Bungay, H.K. Lonsdale, Synthetic Membranes: Science, Engineering, and Applications, Norwell, Boston, 1986.
[2] S. Štandeker, A. Veronovski, Z. Novak, Ž. Knez, Silica aerogels modified with mercapto functional groups used for Cu(II) and Hg(II) removal from aqueous solutions, Desalination 269 (2011) 223–230.
[3] A.K. Meena, G.K. Mishra, P.K. Rai, C. Rajagopal, P.N. Nagar, Removal of heavy metal ions from aqueous solutions using carbon aerogel as an adsorbent, J. Hazard. Mater. 122 (2005) 161–170.
[4] R.J. Kiffs, Surveys in Industrial Wastewater Treatment-Manufacturing and Chemical Industries, Lonngman, New York, 1987.
[5] C. Namasivayam, K. Ranganathan, Removal of Pb(II), Cd(II), Ni(II) and mixture of metal Ions by adsorption onto 'waste' Fe(III)/Cr(III) hydroxide and fixed bed studies, Environ. Technol. 16 (1995) 851–860.
[6] A.K. Geim, Graphene: status and prospects, Science 324 (2009) 1530–1534.
[7] M.I. Katsnelson, Graphene: carbon in two dimensions, Mater. Today 10 (2007) 20–27.
[8] L. Tsetseris, S.T. Pantelides, Graphene: an impermeable or selectively permeable membrane for atomic species? Carbon 67 (2014) 58–63.
[9] Ç.Ö. Girit, J.C. Meyer, R. Erni, M.D. Rossell, C. Kisielowski, L. Yang, C.-H. Park, M.F. Crommie, M.L. Cohen, S.G. Louie, A. Zettl, Graphene at the edge: stability and dynamics, Science 323 (2009) 1705–1708.

[10] M. Klintenberg, S. Lebègue, M.I. Katsnelson, O. Eriksson, Theoretical analysis of the chemical bonding and electronic structure of graphene interacting with group IA and group VIIA elements, Phys. Rev. B: Condens. Matter 81 (2010) 085433.
[11] J. Wu, L. Xie, Y. Li, H. Wang, Y. Ouyang, J. Guo, H. Dai, Controlled chlorine plasma reaction for noninvasive graphene doping, J. Am. Chem. Soc. 133 (2011) 19668–19671.
[12] D.W. Boukhvalov, M.I. Katsnelson, Chemical functionalization of graphene, J. Phys.: Condens. Matter 21 (2009) 344205.
[13] M.Z. Hossain, J.E. Johns, K.H. Bevan, H.J. Karmel, Y.T. Liang, S. Yoshimoto, K. Mukai, T. Koitaya, J. Yoshinobu, M. Kawai, A.M. Lear, L.L. Kesmodel, S.L. Tait, M.C. Hersam, Chemically homogeneous and thermally reversible oxidation of epitaxial graphene, Nat. Chem. 4 (2012) 305–309.
[14] B. Huang, Z. Li, Z. Liu, G. Zhou, S. Hao, J. Wu, B.-L. Gu, W. Duan, Adsorption of gas molecules on graphene nanoribbons and its implication for nanoscale molecule sensor, J. Phys. Chem. C 112 (2008) 13442–13446.
[15] Q.H. Wang, M.C. Hersam, Room-temperature molecular-resolution characterization of self-assembled organic monolayers on epitaxial graphene, Nat. Chem. 1 (2009) 206–211.
[16] A.K. Geim, K.S. Novoselov, The rise of graphene, Nat. Mater. 6 (2007) 183–191.
[17] A.H. Castro Neto, F. Guinea, N.M.R. Peres, K.S. Novoselov, A.K. Geim, The electronic properties of graphene, Rev. Mod. Phys. 81 (2009) 109–162.
[18] K. Nakada, M. Fujita, G. Dresselhaus, M.S. Dresselhaus, Edge state in graphene ribbons: nanometer size effect and edge shape dependence, Phys. Rev. B: Condens. Matter 54 (1996) 17954–17961.
[19] M.D. Stoller, S. Park, Y. Zhu, J. An, R.S. Ruoff, Graphene-based ultracapacitors, Nano Lett. 8 (2008) 3498–3502.
[20] A. Baskin, P. Kral, Electronic structures of porous nanocarbons, Sci. Rep. 1 (2011) 1–7.
[21] S. Blankenburg, M. Bieri, R. Fasel, K. Müllen, C.A. Pignedoli, D. Passerone, Porous graphene as an atmospheric nanofilter, Small 6 (2010) 2266–2271.
[22] S. Garaj, W. Hubbard, A. Reina, J. Kong, D. Branton, J.A. Golovchenko, Graphene as a subnanometre trans-electrode membrane, Nature 467 (2010) 190–193.
[23] R.R. Nair, H.A. Wu, P.N. Jayaram, I.V. Grigorieva, A.K. Geim, Unimpeded permeation of water through helium-leak–tight graphene-based membranes, Science 335 (2012) 442–444.
[24] D.C. Bell, M.C. Lemme, L.A. Stern, J.R. Williams, C.M. Marcus, Precision cutting and patterning of graphene with helium ions, Nanotechnology 20 (2009) 455301.
[25] M. Bieri, M. Treier, J. Cai, K. Ait-Mansour, P. Ruffieux, O. Groning, P. Groning, M. Kastler, R. Rieger, X. Feng, K. Mullen, R. Fasel, Porous graphenes: two-dimensional polymer synthesis with atomic precision, Chem. Commun. (2009) 6919–6921.
[26] M. Kim, N.S. Safron, E. Han, M.S. Arnold, P. Gopalan, Fabrication and characterization of large-area, semiconducting nanoperforated graphene materials, Nano Lett. 10 (2010) 1125–1131.
[27] A.W. Hauser, P. Schwerdtfeger, Nanoporous graphene membranes for efficient ^{3}He/^{4}He separation, J. Phys. Chem. Lett. 3 (2011) 209–213.
[28] J. Schrier, J. McClain, Thermally-driven isotope separation across nanoporous graphene, Chem. Phys. Lett. 521 (2012) 118–124.
[29] J.S. Bunch, S.S. Verbridge, J.S. Alden, A.M. van der Zande, J.M. Parpia, H.G. Craighead, P.L. McEuen, Impermeable atomic membranes from graphene sheets, Nano Lett. 8 (2008) 2458–2462.
[30] A. Hashimoto, K. Suenaga, A. Gloter, K. Urita, S. Iijima, Direct evidence for atomic defects in graphene layers, Nature 430 (2004) 870–873.
[31] M.D. Fischbein, M. Drndić, Electron beam nanosculpting of suspended graphene sheets, Appl. Phys. Lett. 93 (2008) 113107–113109.
[32] T.R. Gaborski, J.L. Snyder, C.C. Striemer, D.Z. Fang, M. Hoffman, P.M. Fauchet, J.L. McGrath, High-Performance Separation of nanoparticles with ultrathin porous nanocrystalline silicon membranes, ACS Nano 4 (2010) 6973–6981.
[33] D.E. Jiang, V.R. Cooper, S. Dai, Porous graphene as the ultimate membrane for gas separation, Nano Lett. 9 (2009) 4019–4024.
[34] M.W. Schmidt, K.K. Baldridge, J.A. Boatz, S.T. Elbert, M.S. Gordon, J.H. Jensen, S. Koseki, N. Matsunaga, K.A. Nguyen, S. Su, T.L. Windus, M. Dupuis, J.A. Montgomery, General atomic and molecular electronic structure system, J. Comput. Chem. 14 (1993) 1347–1363.
[35] E. Lewars, Computational chemistry: introduction to the theory and applications of molecular and quantum mechanics, Springer, New York, 2011.
[36] F. Jensen, Introduction to computational chemistry, John Wiley & Sons, Hoboken, 2007.
[37] C.Y. Won, N.R. Aluru, Water permeation through a subnanometer boron nitride nanotube, J. Am. Chem. Soc. 129 (2007) 2748–2749.
[38] J.J. Sardroodi, J. Azamat, A. Rastkar, N.R. Yousefnia, The preferential permeation of ions across carbon and boron nitride nanotubes, Chem. Phys. 403 (2012) 105–112.
[39] G. Chen, Y. Guo, N. Karasawa, W.A. Goddard III, Electron–phonon interactions and superconductivity in K_{3}C_{60}, Phys. Rev. B: Condens. Matter 48 (1993) 13959–13970.
[40] L. Kalé, R. Skeel, M. Bhandarkar, R. Brunner, A. Gursoy, N. Krawetz, J. Phillips, A. Shinozaki, K. Varadarajan, K. Schulten, NAMD2: Greater scalability for parallel molecular dynamics, J. Comput. Phys. 151 (1999) 283–312.
[41] J. Azamat, J. Sardroodi, The permeation of potassium and chloride ions through nanotubes: a molecular simulation study, Monatsh. Chem. 145 (2014) 881–890.
[42] T. Darden, D. York, L. Pedersen, Particle mesh Ewald: An N·log(N) method for Ewald sums in large systems, J. Chem. Phys. 98 (1993) 10089–10092.
[43] W. Humphrey, A. Dalke, K. Schulten, VMD: Visual molecular dynamics, J. Mol. Graph. 14 (1996) 33–38.
[44] J.C. Phillips, R. Braun, W. Wang, J. Gumbart, E. Tajkhorshid, E. Villa, C. Chipot, R.D. Skeel, L. Kalé, K. Schulten, Scalable molecular dynamics with NAMD, J. Comput. Chem. 26 (2005) 1781–1802.
[45] B.R. Brooks, R.E. Bruccoleri, B.D. Olafson, D.J. States, S. Swaminathan, M. Karplus, CHARMM: A program for macromolecular energy, minimization, and dynamics calculations, J. Comput. Chem. 4 (1983) 187–217.
[46] W.L. Jorgensen, J. Chandrasekhar, J.D. Madura, R.W. Impey, M.L. Klein, Comparison of simple potential functions for simulating liquid water, J. Chem. Phys. 79 (1983) 926–935.
[47] R. Kjellander, H. Greberg, Mechanisms behind concentration profiles illustrated by charge and concentration distributions around ions in double layers, J. Electroanal. Chem. 450 (1998) 233–251.
[48] G.M. Torrie, J.P. Valleau, Nonphysical sampling distributions in monte carlo free-energy estimation: Umbrella sampling, J. Comput. Phys. 23 (1977) 187–199.
[49] A. Grossfield, WHAM: the weighted histogram analysis method, 2014, version 2.0.8, h*ttp://membrane.urmc.rochester.edu/content/wham.
[50] A. Luzar, Resolving the hydrogen bond dynamics conundrum, J. Chem. Phys. 113 (2000) 10663–10675.
[51] J.M. Di Leo, J. Marañón, Confined ions and water in nanotube, J. Mol. Struct. THEOCHEM 709 (2004) 163–166.
[52] R.W. Impey, P.A. Madden, I.R. McDonald, Hydration and mobility of ions in solution, J. Phys. Chem. 87 (1983) 5071–5083.
[53] S.H. Lee, J.C. Rasaiah, Molecular dynamics simulation of ion mobility. 2. Alkali metal and halide ions using the SPC/E model for water at 25 °C, J. Phys. Chem. 100 (1996) 1420–1425.